DESIGN AND CHARACTERISATION OF THE FOCUSING SOLENOIDAL SYSTEM FOR THE CLARA HIGH REPETITION RATE ELECTRON SOURCE

D.J. Scott[#, 1], A.R. Bainbridge[1], R.J. Cash, T.J. Jones, K.B. Marinov[1], B.J.A. Shepherd[1],
B.L. Militsyn[1], STFC ASTeC, Daresbury Laboratory, UK
C.S. Edmonds[1], University of Liverpool, UK
[1]also at The Cockcroft Institute, Warrington, WA4 4AD, UK

Abstract

One of the critical components of electron injectors based on RF photoelectron sources is the focusing system. The system typically consists of a Main Focusing Solenoid and a Bucking Coil. Combination of these two solenoids should provide proper focusing of the beam at the exit of the RF cavity and zero longitudinal magnetic field in the photocathode plane to minimise the beam emittance. Imperfection of the solenoid design, manufacturing and alignment frequently leads to asymmetry of the focusing field which has to be compensated with additional coils. In order to eliminate mechanical and magnetic misalignment the CLARA photoinjector solenoids are mounted on one integrated bench and before installation into the beamline have been aligned in the magnet laboratory with simultaneous measurement of the magnetic field. In order to define multipole field components, dedicated measurements of the transverse magnetic field have been done. The amplitudes of the multipoles have been obtained from analysis of the transverse field map. We present here the results of field characterisation.

MAGNET DESIGN

An overview of the CLARA gun can be found in [1]. The magnetic system of the gun consists of a pair of coaxial, water-cooled solenoids, magnetised in opposite directions such that the fields they generate at the location of the cathode cancel each other out. The bucking solenoid is stationary and the main solenoid can be translated towards and away from the cathode plane. The system is optimised at different solenoid currents and solenoid separations to produce optimum parameters of the emitted beam. The main solenoid is the same design as used on VELA [2], the bucking solenoid had to be specially designed, built and tested. It relies upon an asymmetric steel yoke that shifts the peak axial field away from its geometric centre towards the cathode to allow for a more efficient use of the available Ampere-turns. The design and assembly are shown in Fig. 1.

MAGNETIC CHARACTERISATION

Before installation both solenoids were extensively tested both when operating alone and simultaneously and were found to perform exactly as expected, as the comparison between measurement and simulation field data shown in (Fig. 2).
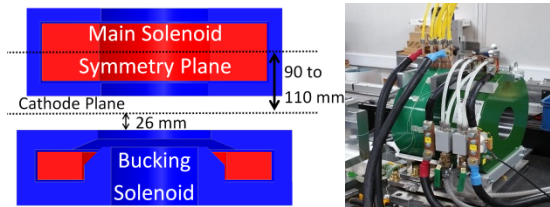
[#] duncan.scott@stfc.ac.uk

Figure 1: The steel yokes are in blue and the magnetising coils are in red. The two solenoids are installed on a Hall probe bench for field measurements.

Main Solenoid Transverse Field Measurements

Measurements were taken with a 3 axis Hall probe at 3 different longitudinal coordinates, 0 and ±10 mm longitudinally and 4 orientations about the longitudinal axis: 0°, 90°, 180°, and 270°. The different orientations were used to correct for any transverse and planar Hall effects. To compare the measurements at different orientations the components of the field vectors should be aligned with the same spatial direction. Nominally, the field vectors are 90° rotations of the (X,Y,Z) axes, however due to alignment errors of the Hall probe each field component for the different orientations has a slightly different spatial direction. The field components can be rotated to an 'objectively defined' direction for each measurement. For example, the direction of maximum B_z, $B_{z,max}$. This axis becomes the nominal Z axis and is assumed to be the same for each measurement set. To achieve this we optimise the Hall probe data with respect to the longitudinal field in the solenoid by maximising:

$$\sum_{n=1}^{m} (0,0,1) \cdot \left(R(\underline{a}, \theta) \cdot \underline{B_n} \right)$$

where $\underline{B_n}$ is the measurement at each point, there are m measurements and we optimise $R(\underline{a}, \theta)$, a rotation matrix of angle θ about an axis $\underline{a}$. Once each measurement is represented in the same coordinate system the measurements can be combined. In practise two rotations are required: the first defines a global rotation axis and angle about which to rotate each measurement point to maximise the global longitudinal field component. The second rotates around $B_{z,max}$ to align the transverse components with the nominal X and Y directions. Figure 3 shows the transverse field.
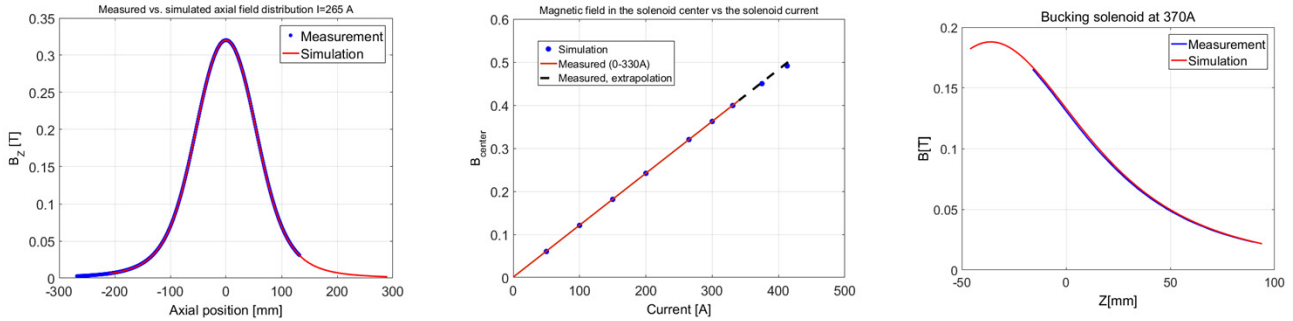
Figure 2: Gun solenoids: measurements vs simulation. (Left) Axial field variation of the main solenoid. (Centre) Excitation curve of the main solenoid. (Right) Axial field variation of the bucking solenoid.
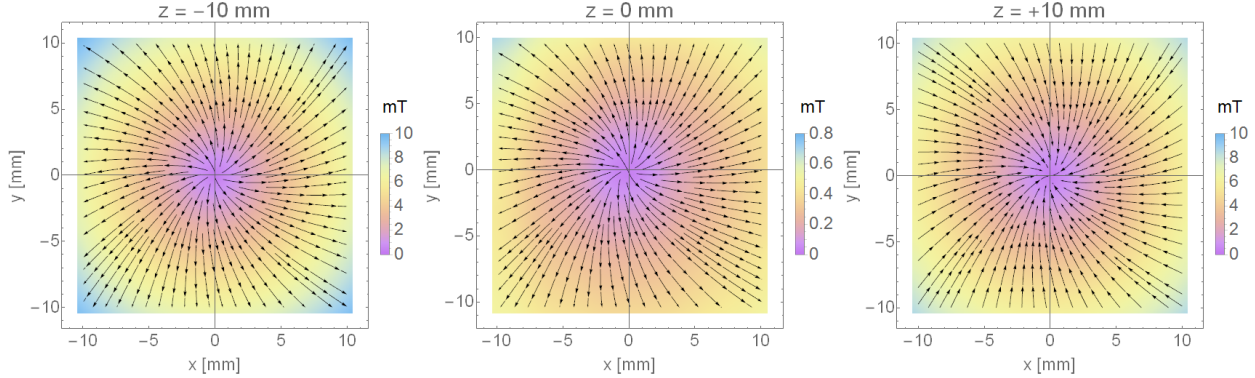

Figure 3: Measured transverse field direction and magnitude at the nominal longitudinal centre of the solenoid (z=0 mm) and 10 mm upstream (z=+10mm) (i.e. towards the cathode) and -10mm downstream (z=-10 mm).

Main Solenoid Transverse Field Multipoles

Magnetic fields are derived from a potential function which is the solution to the Laplace equations, expressed as a series expansion in the complex plane. The normal and skew components of each multipole are given by the real and imaginary parts of the expansion coefficients. The Laplacian can be expanded in different curvilinear coordinate systems; we consider the polar basis with transverse coordinates (r, θ). The 2D representation is only valid in the body of a long magnet with constant longitudinal field. The measured longitudinal variation in the solenoid over the area to be considered is ~1% and so we assume the following is valid. The transverse field components of a magnetic field $\boldsymbol{B}$ can be represented by the following well-known expansions:

$$B_\theta + iB_r = \sum_{n=1}^{\infty} C_n r^{n-1} e^{in\theta}$$

Here n is the order of the multipole, $n = 1$ is a dipole, $n = 2$ is a quadruple etc. The C_n represent the magnitude of the normal and skew components of each multipole. For a discrete set of magnetic field measurements the C_n can be found with a Discrete Fourier Transform in the polar basis. We make M measurements at constant radius r, varying the polar angle θ from 0 to $2\pi \frac{p}{M}$, where $p = 0, 1, 2, 3 \dots M - 1$. The field at each θ_p can be represented by the complex number $B_p = B_\theta + i\, B_r$

giving the C_n as:

$$C_n = \frac{1}{Mr^{n-1}} \sum_{p=0}^{M-1} B_p e^{-2\pi in\frac{p}{M}}$$

An advantage of using the polar basis is that the basis functions, of the form $e^{-in\theta}$, are orthogonal for integer n, guaranteeing each C_n is independent. The units of C_n depend on the units of r and B. The multipole components are calculated by taking the transverse field components at a fixed radius r and varying θ from 0 to 2π. This can be done by interpolating the measured field. Presently, this has been done with a simple spline guaranteeing continuous derivatives that provides an approximation to the Maxwell equations. The accuracy of $C_n, \Delta C_n$ scales with the accuracy of $B_p, \Delta B_p$ as:

$$\Delta C_n \sim \frac{\Delta B_p}{r^{n-1}}$$

the greater the chosen r the greater the accuracy in C_n. We choose $r = 9.9$ mm to give the greatest possible radius. The relative error in the Hall probe measurements are 0.5%, the error in the position of the probe is of the order of a micron and so we assume it is negligible. The convergence of the C_2 as M is increased is shown in Fig. 4, and final results for each C_2 in Table 1.
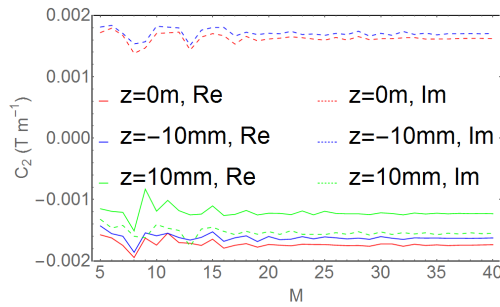
Figure 4 C_2 for increasing M for the three field maps.

Table 1: Real (Re) and Imaginary (Im) Parts of C_2

Parameter	Unit	Value
Z position	mm	-10, 0, 10
M	-	40, 40, 40
Re(C_2)	mT/m	-2.3, -1.7, -1.2
Im(C_2)	mT/m	4.4, 1.6, -1.6

DESIGN AND CHARACTERISATION OF THE INTEGRATED FOCUSING SYSTEM

The solenoids and injector each sit on an independent support systems, (Fig.5). The base of the solenoid support plate is a 'U' shape and the base of the injector support plate a 'T', the two supporting systems are designed such that the installation of the combined solenoid assembly allows offline magnetic alignment in the magnet laboratory.
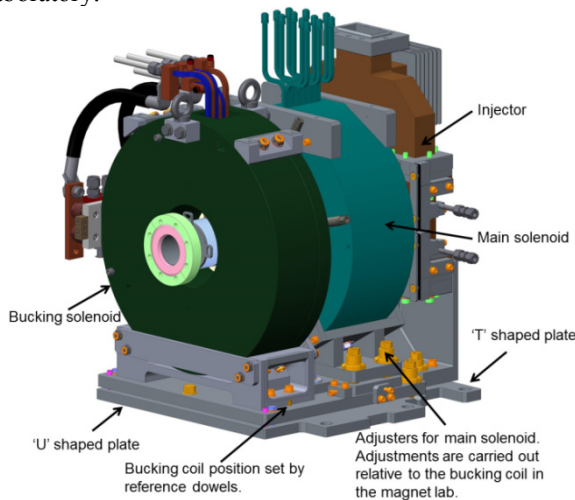

Figure 5: Solenoids support system.

Alignment in the magnet laboratory is carried out by measuring the transverse field centre in x and y at several points along the axis of each solenoid magnet. The centre is calculated by minimising the longitudinal field B_z. Following this, the main solenoid can be moved in x and y to align the axis with that of the bucking solenoid. Figure 6 shows the horizontal and vertical positions of the magnets after the final adjustment. This alignment is then maintained during subsequent installation of the solenoids around the injector in the accelerator hall.
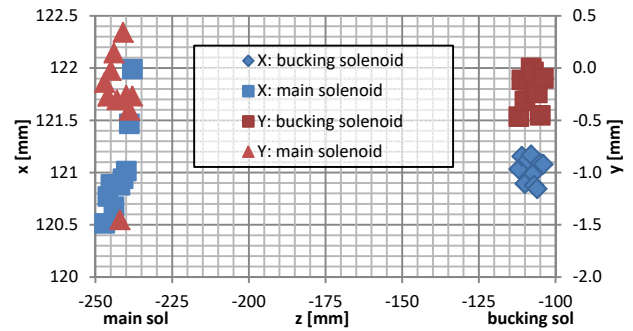

Figure 6: Final positions of solenoids after alignment.

SIMULATED IMPACT ON THE BEAM

We use GPT [3] to investigate the impact of non-solenoidal skew multipole terms on the emittance measured 1 m downstream of the cathode. Within the simulation, a skew quadrupole of 20 cm in length (starting at the position of the cathode surface) is superposed on to the solenoid field map. The simulation, which includes a space charge model, as well as 2.5 D cylindrically symmetric field maps for the solenoids and RF cavity, is run for skew quadrupole gradients ranging from -6 mT/m to 6 mT/m. In Fig. 7, we show the normalised horizontal and vertical emittance calculated at the reference position vs the skew quadrupole gradient. The introduced skew multipole terms lead to small changes in the ratio of the horizontal to vertical emittance, however more work is required to understand the impact of this level of asymmetry. The measurements indicate skew quadrupole terms that vary significantly over the 20 mm measurement range, the simulations include terms that are constant over 20 cm, therefore it's likely the simulations overestimate the impact of the measured terms. Asymmetries in the laser spot should also be considered in future studies.
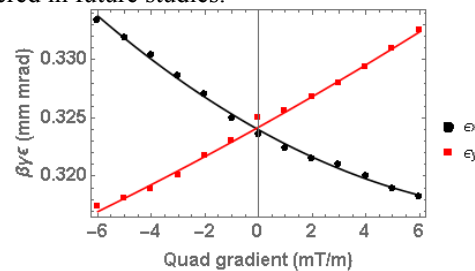

Figure 7: Normalised horizontal and vertical emittance at the reference position vs the skew quadrupole gradient.

REFERENCES

[1] B.L. Militsyn *et al.*, "Status of the Injector System For The CLARA FEL Test Facility", In Proc. of Linear Accelerator Conference (LINAC'16), East Lansing, USA, September 2016, pp. 167-170.

[2] F. Kiewiet, Ph. D. Thesis, Eindhoven University of Technology, 2003.

[3] S. B. van der Geer, O. J. Luiten, M. J. de Loos, G. Pöplau, U. van Rienen, 3D space-charge model for GPT simulations of high brightness electron bunches, Institute of Physics Conference Series , vol. 175, p. 101, 2005.